Structural Engineering and Mechanics, Vol. 35, No. 1 (2010) 19-35
DOI: http://dx.doi.org/10.12989/sem.2010.35.1.019

A hybrid simulated annealing and optimality criteria method for optimum design of RC buildings

Gang Li[1]*, Haiyan Lu[2] and Xiang Liu[1]

[1]*Department of Engineering Mechanics, State Key Laboratory of Structural Analysis of Industrial Equipment, Dalian University of Technology, Dalian, 116024, China*
[2]*School of Architecture & Civil Engineering, Shenyang University of Technology, Shenyang, 110023, China*

(Received April 30, 2008, Accepted December 28, 2009)

Abstract. This paper proposes a hybrid heuristic and criteria-based method of optimum design which combines the advantages of both the iterated simulated annealing (SA) algorithm and the rigorously derived optimality criteria (OC) for structural optimum design of reinforced concrete (RC) buildings under multi-load cases based on the current Chinese design codes. The entire optimum design procedure is divided into two parts: strength optimum design and stiffness optimum design. A modified SA with the strategy of adaptive feasible region is proposed to perform the discrete optimization of RC frame structures under the strength constraints. The optimum stiffness design is conducted using OC method with the optimum results of strength optimum design as the lower bounds of member size. The proposed method is integrated into the commercial software packages for building structural design, SATWE, and for finite element analysis, ANSYS, for practical applications. Finally, two practical frame-shear-wall structures (15-story and 30-story) are optimized to illustrate the effectiveness and practicality of the proposed optimum design method.

Keywords: reinforced concrete structure; strength; stiffness; simulated annealing; optimality criteria.

1. Introduction

For a reinforced concrete building whose topology and shape are fixed, the main task of the structural engineer is to determine the size of the member cross section and the area of reinforcement. The structural engineer can obtain the structural responses subjected to multi-load cases by a number of available software packages, which, however, can not provide the direct methods to modify the member size and reinforcement area automatically to satisfy specific regulations of the design codes. The structural member dimensions and reinforcement area have to be determined by the designer mainly based on design experiences, in which the final design project may be uneconomical or even unacceptable. Thus, a design method based on structural optimization becomes necessary.

In recent years, many activities have been reported in literature on the development of drift control algorithm based on structural optimization. Chan *et al*. (1997, 2001, 2004) developed an

*Corresponding author, Professor, E-mail: ligang@dlut.edu.cn

efficient computer-based optimization technique for lateral stiffness design of tall buildings. Cheng and Li (1998) presented the reliability-based structural optimization under hazard loads, in which the framework and frame shear-wall structure under multi-loads were considered. Li *et al*. (1999) proposed multi-objective and multi-level optimization techniques for steel frames, in which two levels of system and element, two objectives of maximization of the total structural strain energy and minimization of the total structural weight were considered. Park and Sung (2002) presented a distributed simulated annealing (SA) algorithm for optimal structural design for steel structures under maximum displacement and inter-story drift constraints. Park *et al*. (2002, 2003) presented the stiffness-based resizing techniques for the drift optimal design of steel-frame and shear-wall systems for tall buildings. Gong *et al*. (2005) studied sensitivity analysis of performance-based design for steel moment frames. Zou *et al*. (2007) developed a multi-objective optimization technique that incorporates the performance-based seismic design methodology of concrete building structures, in which the life-cycle cost is minimized subject to multiple levels of seismic performance design criteria. Although all of the cited methods are successfully applied to drift control of tall building structures, these methods are not capable of the strength design of structures. Moreover, all these stiffness optimizations are carried out using continuous variables; practical application of these solutions, however, requires additional modifications to meet the discrete nature of structural design variables.

The optimal design of reinforcement in beam or column sections has been presented by several researchers, in which the optimal steel area of reinforcement was obtained to ensure the cross section with adequate resistance to the combined flexural and axial loads. Ferreira *et al*. (2003) studied the optimization of the area and location of steel bars in a T-beam under bending moment, and developed the analytical optimal method for the ultimate design of the reinforcement of T-section. Hernondez-montes *et al*. (2004, 2005) proposed that the required reinforcement of cross section was determined as a function of the neutral axis depth. Aschheim *et al*. (2007) presented an optimal domain approach which provided a direct solution for the optimal reinforcement of rectangular section subjected to the axial and flexural loads in terms of the ultimate design. Chen *et al.* (2002) developed a dynamic optimization mathematical model of engineering structures with the probability constraints of forbidden frequency domain and the vibration mode. Guan (2005) presented an optimization approach for the design of deep beams with web openings. However, all these methods were applied to simple beams and columns with continuous design variables.

Because of the requirements for the discrete size of cross-sections of building structures, the practical discrete optimization techniques are necessary. Simulated annealing (SA) originates from the theory of statistical mechanics, with an analogy to the physical process of annealing a metal (Metropolis *et al.* 1953, Kirpatrick *et al*. 1983, Aarts and Laarhoven 1987). tool ion on tural characteristics and design. As one of the widely used heuristic approaches to solve combinatorial problems, SA can produce a good local though not necessarily global optimal solution within a reasonable computing time. The SA technique was used as a tool to approximate the solution of very large combinatorial optimization problems (Parks 1990). Recently, the SA technique was applied in the discrete optimization of building structures. Balling and Yao (1997) optimized three-dimension reinforced concrete frames using the SA algorithm with a multi-level method, in which discrete variables as well as limits on the number of reinforcing bars and their topological arrangements are considered. Pantelides and Tzan (1997) proposed a modified iterated SA algorithm for optimal design of the structure system with dynamic constraints, and two new strategies, sensitivity analysis and automatic reduction of the feasible region were developed in their studies.

Mohan and Arvind (2007) dealt with optimal stacking sequence design of laminate composite structures using SA. All the cited methods are applied to local strength optimal problems under one or two simple load cases, without considering the lateral stiffness requirements, which may be unfeasible for a practical building design.

In an attempt to improve the current design practice, a hybrid heuristic and criteria-based method of optimum design for RC buildings under multi-load cases is presented. The entire optimum design procedure is divided into strength optimum design and stiffness optimum design, which are performed by the iterated simulated annealing algorithm and the rigorously derived optimality criteria, respectively. A strategy of adaptive feasible region in the SA algorithm is proposed to perform the discrete optimization of RC frame structure under the strength constraints. The proposed method is integrated into the commercial software packages for building structural design, SATWE, and for finite element analysis, ANSYS, for practical applications.

2. Strength optimum design problem under multi-load cases

2.1 Optimum formulation

The aim herein is to design a reinforced concrete frame that minimizes the structural cost. Fig. 1 shows the typical reinforced concrete beam and column with the cross-section width of b, the depth of h and the reinforcement area of A_s. The optimum formulation can be written as

Find member size (b, h)

$$\text{Minimize: } F = \sum_{elements} (C_c \times l \times b \times h + C_s \times l \times A_s + 2C_f \times (b+h) \times l) \tag{1}$$

Subject to

Flexural strength $$M_u \le \phi M_n \tag{2}$$

Axial force strength $$P_u \le \phi P_n \tag{3}$$

Reinforcement ratio $$\rho_{\min} \le \rho = \frac{A_s}{bh} \le \rho_{\max} \tag{4}$$

Axial compression ratio (for column) $$U_{\min} \le U = \frac{P}{f_C bh} \le U_{\max} \tag{5}$$

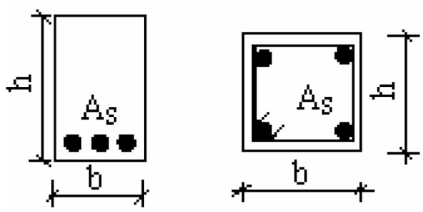

Fig. 1 Typical section of reinforced concrete beam and column

Shear strength $$bh_0 \geq \frac{V}{(0.25\beta_c f_c)} \tag{6}$$

Section size $$h_{\min} \leq h \leq h_{\max}, b_{\min} \leq b \leq b_{\max} \tag{7}$$

where, the cross-sectional dimensions of the member, b and h, are design variables; l *is* the length of the member; C_c, C_s and C_f are the unit cost of concrete, steel and formwork, respectively; A_s is the area of tension reinforcement of the member cross-section, h_0 is the effective depth of the member cross-section. P_u is the factored axial strength; P_n is the nominal axial strength of the section; M_u is the factored bending moment, M_n is the nominal flexural strength of the section; $\rho_{\min}$ and $\rho_{\max}$ are the minimum and maximum allowable reinforcement ratios of the member cross-section, respectively; ρ is reinforcement ratio at balanced condition; $U_{\min}$ and $U_{\max}$ are the lower and upper bounds of the axial compression ratio of the column; U is the column axial compression at balanced condition; P is the axial compression design force of the column under multi-loads cases, $\beta_c = 1.0$, V is the shear force of the section, f_c is the compression strength of concrete.

2.2 Review on SA algorithm

The SA algorithm employs a random search which not only accepts the change that decreases the objective function, but also some changes that increase it. In fact, the SA algorithm can be regarded as a “randomized variation” of the local search method. The basic idea of local search is an iterative improvement process, which starts with an initial solution and searches a solution neighborhood with a lower cost solution. If one is found, it replaces the current solution and the search continues. Otherwise, the algorithm returns a locally optimal solution. The process of SA can be summarized in the following steps:

(1) Choose an initial configuration of the solution, C_i, randomly or by some other heuristic method from the initial design region (S^0), with the corresponding objective function $f_i = F(C_i)$.

(2) Generate a random change in the initial configuration, and obtain a new possible configuration C_{i+1}.

(3) Calculate the objective function and the accepted probability (p)
If f_{i+1} is less than f_i, then the change is always accepted (e.g., $p = 1$).
If f_{i+1} is larger than f_i, then the change is accepted with a probability of $p = \exp((f_{i+1} - f_i)/T)$.

(4) Conduct an annealing schedule which provides an initial rule for lowering it as the search processes (such as $T_{i+1} = k * T_i$, $0 < k < 1$, i.e., between zero and one).

(5) Check the termination condition.
Extensive literature about the SA algorithm can be referenced in Aarts *et al.* (1987).

2.3 Modified SA algorithm

In the conventional SA algorithm shown previously, the new solution is stochastically generated from the initial design region which is fixed in the whole optimization process. For the optimal design of building structures, it is often difficult to obtain the feasible region satisfying all constraints using the general trial and error approachespecially for the complex tall building structures. Thus, some modifications may be necessary for its implementation to the specific problems. In this paper, considering the fact that the internal forces in the structure are insensitive to the resizing process, which reflects the particular behavior of tall buildings in general (Chan and Sun 1997), an strategy of adaptive feasible region based on the axial compression ratio, reinforcement ratio and local strength constraints is proposed. For the *k*th beam or column, the design strength (moment M, axial compression N and shear force V), reinforcement ratio (ρ), axial compression ratio (U) can be obtained after the structural analysis at the *n*th iteration. Fix the above obtained design internal forces, section reinforcement ratios and axial compression ratios, a defined region (S_k^n) for each constraint of Eqs. (2)-(7) can be obtained, and then a adaptive feasible region (S_k^n) satisfying all constraints can be generated by simple set operation for all S_k^n (k = 1, 2, 3, ...). Consider the rectangular beam with fixed width and the square column, which have the initial design region $S_k^0 = (h_{k\min}^0, h_{k\max}^0)$, the procedure to generate the adaptive feasible region is shown as followings.

(1) Let $S_{1,k}^n = (h_{1\min}^n, h_{1\max}^n)$ be the region satisfying the constraint of reinforcement ratio at the *n*th iteration.

Calculate the rate of the column and beam reinforcement ratios: $\gamma_{\min}^n = \rho^n/\rho_{\max}$, $\gamma_{\max}^n = \rho^n/\rho_{\min}$, where ρ^n is the reinforcement ratio of the *n*th iteration.

For a square column, $h_{1\min} = h_k^{n-1}\sqrt{\gamma_{\min}^n}$, $h_{1\max} = h_k^{n-1}\sqrt{\gamma_{\max}^n}$; for a beam $h_{1\min} = h\times\gamma_{\min}^n$, $h_{1\max} = h\times\gamma_{\min}^n$. If $h_{1\min}^n < h_{k\min}^0$ then $h_{1\min}^n = h_{k\min}^0$; and if $h_{1\max}^n > h_{k\max}^0$ then $h_{1\max}^n = h_{k\max}^0$.

(2) Let $S_{2,k}^n = (h_{2\min}^n, h_{2\max}^n)$ be the region satisfying the constraint of axial compression ratio at the *n*th iteration.

Calculate the rate of the column axial compression ratio: $\gamma_{\min}^n = U^n/U_{\max}$, $\gamma_{\max}^n = U^n/U_{\min}$, where U^n is the axial compression ratio of the *n*th iteration.

For a square column, $h_{2\min}^n = h_k^{n-1}\sqrt{\gamma_{\min}^n}$, $h_{2\max}^n = h_k^{n-1}\sqrt{\gamma_{\max}^n}$. If $h_{2\min}^n < h_{k\min}^0$ then $h_{2\min}^n = h_{k\min}^0$ and if $h_{2\max}^n > h_{k\max}^0$ then $h_{2\max}^n = h_{k\max}^0$.

(3) Let $S_{3,k}^n = (h_{3\min}^n, h_{3\max}^n)$ be the region satisfying the constraint of shear strength at the *n*th iteration.

Calculate the rate of shear strength: $\gamma_{\min}^n = V^n/(0.25 f_c bh)$,
where, V^n is the shear strength of the *n*th iteration.

For a square column, $h_{3\min}^n = h_k^{n-1}\gamma_{\min}^n$, $h_{3\max}^n = h_{k\max}^0$. If $h_{3\min}^n < h_{k\min}^0$ then $h_{3\min}^n = h_{k\min}^0$.

(4) Let $S_k^n = (h_{\min}^n, h_{\max}^n)$ be the region satisfying all constraints of Eqs. (2)-(7), which can be expressed as

$$h_{\min}^n = \max\{h_{1\min}^n, h_{2\min}^n, h_{3\min}^n\},\ h_{\max}^n = \min\{h_{1\max}^n, h_{2\max}^n, h_{3\max}^n\} \tag{8}$$

If $h_{\min}^n > h_{\max}^n$ then $h_{\min}^n = h_{\max}^n$.

Fig. 2 shows the flow chart of the SA algorithm for solving structural optimization problems.

3. Stiffness optimum design problem

Consider a reinforced concrete framework with i = 1, 2, ..., n beam and column members, the shear walls and floor slabs are not treated as design variables. The minimum cost design of the RC frame under multi-load cases can be generally stated as

Find: member size (b_i, h_i)

Minimize
$$F = \sum_{i=1}^{n}(w_i b_i h_i l_i) \tag{9}$$

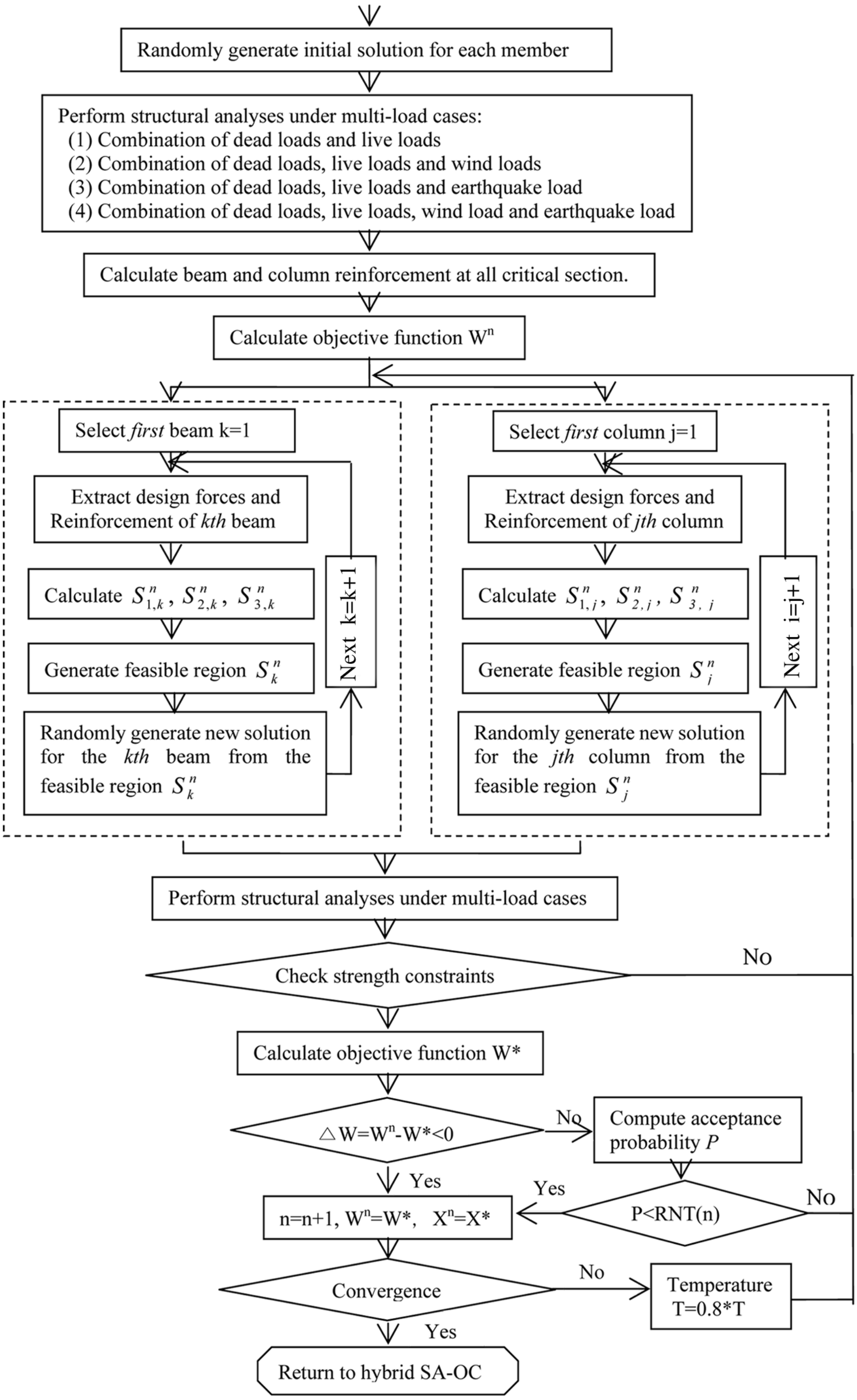

Fig. 2 Flowchart of simulated annealing algorithm

Subject to $$d_i \le d_i^u \qquad (j = 1, 2, \ldots, t) \tag{10}$$

$$b_i^L \le b_i \le b_i^U \qquad (i = 1, 2, \ldots, n) \tag{11}$$

$$h_i^L \le h_i \le h_i^U \qquad (i = 1, 2, \ldots, n) \tag{12}$$

where, w_i is the synthetic unit cost of column or beam, w_i = 85.65 US\$/m^3 according to Chinese code; d_j and d_i^u are the lateral drift and its corresponding allowable limit; t is the number of floors. Eqs. (11) and (12) define the lower and upper bounds of the section width b and depth h, in which the lower bound is determined by the strength optimum design.

To facilitate a numerical solution of the above design optimization problem, the implicit drift constraints must be formulated explicitly in terms of design variables b_i and h_i. From the virtual work, the drift constraints can then be formulated explicitly as

$$d_j = \sum_{i=1}^{s}\left(\frac{E_{0ij}}{b_i h_i} + \frac{E_{1ij}}{b_i h_i^3} + \frac{E_{2ij}}{b_i^3 h_i}\right) \qquad (j = 1, 2, \ldots, t) \tag{13}$$

where, $E_{0ij}, E_{1ij}, E_{2ij}$ are the virtual strain energy coefficients due to axial and shear forces, flexural moments, and tortional moments for the ith beam or column, respectively, which can be written as

$$E_{0ij} = \int_0^{L_x}\left(\frac{F_x f_x}{E} + \frac{6F_y f_y}{5G} + \frac{6F_z f_z}{5G}\right)d_x, \quad E_{1ij} = \int_0^{L_i}\left(\frac{12M_z m_z}{E}\right)d_x, \quad E_{2it} = \int_0^{L_i}\left(\frac{M_x m_x}{\beta G} + 12\frac{M_y m_y}{E}\right)d_x$$

where, L_i is the length of member i, E and G are the axial and shear elastic material moduli, $\beta \approx 0.2$ for typical rectangular sections; $F_x, F_y, F_z, M_x, M_y, M_z$, are the nth modal member axial force, shear force, torque and bending moment; $f_x, f_y, f_z, m_x, m_y, m_z$ are member axial force, shear force, torque and bending moment due to a unit virtual load applied to the building at the location corresponding to the combined drift d_i^u.

In the OC method, the constrained optimization problem is first transformed into an unconstrained one of a Lagrangian function which involves the objective function and the explicit drift constraints associated with corresponding Lagrangian multipliers. Then, a set of necessary optimality criteria for the optimal design is derived from the stationary conditions of the Lagrangian function. Based on the derived optimality criteria, a linear recursive relation to resize design variable of section width b and depth h can be developed as follows (Chan *et al*. 1997, 2001, 2004).

$$b_i^{v+1} = b_i^v\left\{1 + \frac{1}{\eta}\left(\sum_{j=1}^{t}\frac{\lambda_j^v}{l_i}\left(\frac{E_{0ij}}{b_i^2 h_i^2} + \frac{E_{1ij}}{b_i^2 h_i^4} + \frac{3E_{2ij}}{b_i^4 h_i^2}\right) - 1\right)\right\} \tag{14}$$

$$h_i^{v+1} = h_i^v\left\{1 + \frac{1}{\eta}\left(\sum_{j=1}^{t}\frac{\lambda_j^v}{l_i}\left(\frac{E_{0ij}}{b_i^2 h_i^2} + \frac{3E_{1ij}}{b_i^2 h_i^4} + \frac{E_{2ij}}{b_i^4 h_i^2}\right) - 1\right)\right\} \tag{15}$$

where v denotes the current iteration number, η (0.5~0.9) is a relaxation parameter which can be adaptively adjusted to control the rate of convergence and λ_j^v presents Lagrangian multipliers for the corresponding the jth drift constraint.

Before Eqs. (14) and (15) can be used to resize the design variables b_i and h_i, the Lagrangian multipliers λ_j must first be determined. Considering the sensitivity of the jth drift constraint with respect to the design variables, one can derive a set of t simultaneous equations to solve λ_j as (Chan *et al.* 1997, 2001, 2004)

$$\sum_{j=1}^{t}\lambda_j\left\{\begin{array}{c}\displaystyle\sum_{i=1}^{n}\frac{1}{w_i b_i^3 h_i^3}\left(E_{0ij}+\frac{E_{1ij}}{h_i^2}+\frac{3E_{2ij}}{b_i^2}\right)\left(E_{0ik}+\frac{E_{1ik}}{h_i^2}+\frac{3E_{2ik}}{b_i^2}\right)\\ \displaystyle+\sum_{i=1}^{n}\frac{1}{b_i h_i}\left(E_{0ik}+\frac{E_{1ik}}{h_i^2}+\frac{3E_{2ik}}{b_i^2}\right)\sum_{i=1}^{n}\frac{1}{b_i h_i}\left(E_{0ik}+\frac{3E_{1ik}}{h_i^2}+\frac{E_{2ik}}{b_i^2}\right)\end{array}\right\} \tag{16}$$
$$=-\eta(d_k^U-d_k^v)+\sum_{i=1}^{n}\frac{1}{b_i h_i}\left(E_{0ik}+\frac{E_{1ik}}{h_i^2}+\frac{3E_{2ik}}{b_i^2}\right)\sum_{i=1}^{n}\frac{1}{b_i h_i}\left(E_{0ik}+\frac{3E_{1ik}}{h_i^2}+\frac{E_{2ik}}{b_i^2}\right)\quad (k=1,2,\ldots,t)$$

Thus, the OC procedure can be described as follows. From the current sizing variables b_i^v and h_i^v, the corresponding λ_j^v values are readily determined by the solving the simultaneous Eq. (16) Having the current values of λ_j^v, the new set of design variables b_i^{v+1} and h_i^{v+1} can then be obtained by the respective relations Eqs. (14) and (15). By successively applying the above recursive optimization algorithm until convergence occurs, the solution for the stiffness optimization is then found.

4. The hybrid SA-OC method

This paper proposes a hybrid heuristic and criteria-based method of optimum design, which combines the advantages of both the iterated simulated annealing (SA) algorithm and the rigorously derived optimality criteria (OC) for structural optimum design of reinforced concrete buildings under multi-load cases, to form a method capable of solving practical building design problems with a large number of elements under strength and lateral stiffness constraints. The SA algorithm does not need gradient computations, and can handle discrete design variables. The OC method has been shown to be particularly efficient in element resizing design of large-scale building structures under stiffness constraints (Chan *et al*. 1997, 2001, 2004). A pseudo-discrete technique (Jasbir 1997) is used in OC method to transform the continuous design variables to the discrete ones.

Fig. 3 depicts an overview of the hybrid SA-OC method for optimum design of RC buildings.

5. Applications to high building structural design

5.1 A 15-story RC frame

A practical 15-story frame (as shown in Fig. 4) is optimized using the proposed hybrid SA-OC method. According to the construction requirement, the building is divided into three standard levels, 1-5 stories, 6-10 stories and 11-15 stories. The concrete compression strength f_c is 14.3 Mpa and the steel strength fy is 300 Mpa for all members. The density of concrete is 25.0 kN/m^3. The

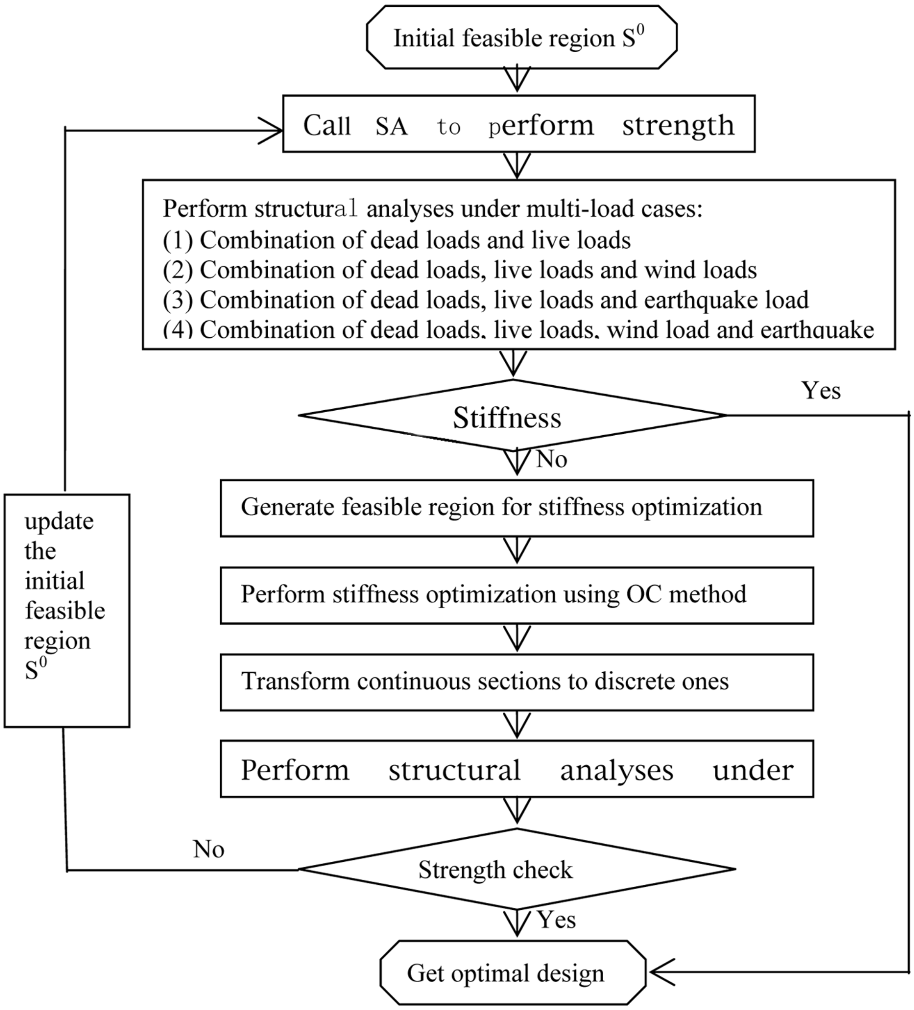

Fig. 3 Flowchart of developed hybrid SA-OC method

dead loads of 3.5 kN/m^2 and 5.0 kN/m^2 are applied to the floor slab and the roof, respectively. The live loads for the floor slab and roof are 2.0 kN/m^2 and 0.7 kN/m^2. Seismic loads were determined according to the Chinese building code (GB50011-2001) with a peak acceleration of 0.08 g, and the characteristic period of site is taken as Tg = 0.25s. The allowable value of the elastic inter-story drift ratio is 1/800. The allowable range of the column axial compression ratio is between 0.5 and 0.6. The allowable range of reinforcement ratio is between 0.8% and 1.5%. The wind load was determined according to the Chinese building code (GB5009-2001), and the standard wind pressure is 0.7 kN/m^2. The initial size is chosen as 250 mm × 250 mm for columns and 250 mm × 300 mm for beams. Beams and columns are designed in groups in each standard level, 6 groups for beams and 4 groups for columns, shown in Fig. 4. The column is assumed to square-shaped and the width for all beam is fixed, b = 250 mm. The unit cost of concrete, steel, and formwork is estimated as C_c = 100 US$/m^3, C_s = 550 US$/ton, and C_f = 1.6 US$/m^2, respectively.

Considering the construction requirements, the allowable cross-sections of beams or columns of

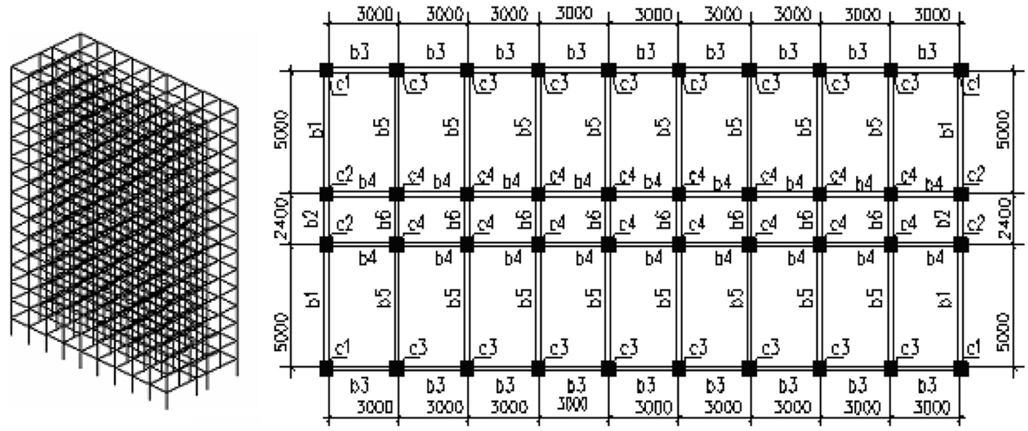

Fig. 4 Vertical plan, standard layout and member group of 15-story RC frame

Table 1 Initial design region S^0 of beam and column

Number of design section	1	2	3	4	...	15	16	17	...	30	31	32
Beam section depth (mm)	300	325	350	375	...	650	675		...			
Column section depth (mm)	225	250	275	300	...	575	600	625	...	970	975	1000

Table 2 Feasible section S^2 of beam and column

Number of member	Reinforcement ratio constraint and candidate sections		Axial compression ratio constraint and candidate sections		Shear constraint and candidate sections		Adaptive Feasible region	
	ρ^2 (%)	S_1^2 ($h_{1\min}$, $h_{1\max}$)	U^2	S_2^2 ($h_{2\min}$–$h_{2\max}$)	V^2 (kN)	S_3^2 ($h_{3\min}$–$h_{3\max}$)	S^2 ($h_{\min}$–$h_{\max}$)	Number of candidate sections
*b*1	3.93	675, 675			90	300-675	675-675	1
*b*2	2.91	675-675			93	300-675	675-675	1
*b*3	0.98	300-367			34	300-675	300-367	3
*b*4	1.05	300-393			40	300-675	300-393	4
*b*5	4.25	675-675			98	300-675	675-675	1
*b*6	2.96	675-675			98	300-675	675-675	1
*c*1	6.2	516-775	0.85	354-425	54	225-1000	516-516	1
*c*2	5.9	491-737	0.83	345-415	71	225-1000	491-491	1
*c*3	6.5	541-812	1.04	433-520	71	225-1000	541-541	1
*c*4	6.4	533-800	1.09	454-545	71	225-1000	533-545	2

the building structures are discrete and distributed in a relatively small available region. Table 1 lists the candidate sections for all columns and beams in the initial design region S^0, which is generated according to the experience of designers. The number of sections in S^0 is 16 and 32 for each beam and column, respectively. Thus, the size of the initial design region turns out to be $16^6 \times 32^4$ for the structure.

Following the adaptive strategy of feasible region, the size of the feasible sections is updated for each beam and column during iteration of SA algorithm. Table 2 lists the candidate sections for all beams and columns after the first iteration. Comparing Table 1 and Table 2, the number of candidate sections in S^2 is 1,1,3,4,1,1 for beams, and 1,1,1,2 for columns, respectively. Thus the size of the feasible region for the structure is $3 \times 4 \times 2 = 24$, reducing the size of the initial design region considerably, which indicates that the technique of adaptive feasible region can improves the efficiency of SA algorithm a lot, and makes it available to optimum design of complicated building structures.

Fig. 5 presents the optimal iteration history of both the strength and stiffness optimum designs. In the strength optimum design, because the SA algorithm accepts not only the design with a lower objective function, but also the design with a relatively larger objective function with a certain probability at each iteration, there exist some intermediate iterations, at which the cost increases. The optimal design process converges steadily after 8 design iterations. In the stiffness optimization design, because the member force distribution is somewhat insensitive to the changes of member size and the strength optimal results have been taken as lower boundaries of member size, the convergence of the stiffness optimum design has been achieved after 5 iterations. In the strength optimization under multi-loads, the structural cost increases from initial US$271662 to the final US$518224. In the stiffness optimization, the inter-story drift constraints are satisfied by changing the member dimensions and reinforcement areas, resulting in the final structural cost of US$522982. By successively applying the above recursive optimization algorithm until convergence occurs, the solution satisfying the strength and stiffness constraints is then found over 24 iterations.

Table 3 presents the member size and the steel area of the initial and optimum designs. Fig. 6 shows the inter-story drift ratios of the initial design under earthquake load, strength optimum design, and stiffness optimum design, respectively. In the initial design, the maximum story drift ratios in x and y direction are 1/700 and 1/300, violating the allowable inter-story drift ratio of 1/800. After the strength optimum design, the maximum drift ratio in x direction is less than 1/800, but the value in y direction still exceeds 1/800. Finally, after the stiffness optimum design, the structure members are resized and the maximum story drift ratios in both x and y directions satisfy

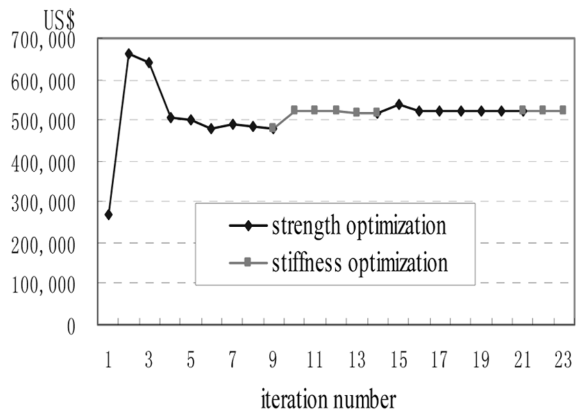

Fig. 5 Optimization history

Table 3 Member size and reinforcement area

Story level	Group	Initial design			Strength optimal design			Stiffness optimal design		
		Width (mm)	Depth (mm)	Steel area (mm^2)	Width (mm)	Depth (mm)	Steel area (mm^2)	Width (mm)	Depth (mm)	Steel area (mm^2)
1-5	b1	250	300	615	250	550	688	250	550	710
	b2	250	300	150	250	500	356	250	500	356
	b3	250	300	202	250	300	234	250	300	236
	b4	250	300	277	250	350	316	250	350	322
	b5	250	300	1020	250	700	1133	250	700	1176
	b6	250	300	150	250	800	645	250	800	776
6-10	b1	250	300	502	250	450	562	250	450	583
	b2	250	300	150	250	400	354	250	400	378
	b3	250	300	180	250	300	207	250	300	212
	b4	250	300	255	250	300	290	250	300	299
	b5	250	300	907	250	850	1007	250	850	1049
	b6	250	300	150	250	500	374	250	550	378
11-15	b1	250	300	435	250	450	486	250	450	503
	b2	250	300	150	250	300	187	250	300	187
	b3	250	300	150	250	300	187	250	300	187
	b4	250	300	225	250	300	255	250	300	261
	b5	250	300	840	250	450	931	250	450	938
	b6	250	300	150	250	300	187	250	300	187
1-5	C1	250	250	2587	300	300	2327	350	350	2527
	C2	250	250	2493	350	350	2720	400	400	2820
	C3	250	250	2268	400	400	2835	450	450	2875
	C4	250	250	2741	400	400	3645	450	450	3735
6-10	C1	250	250	2443	300	300	2070	300	300	2358
	C2	250	250	2475	300	300	2079	300	300	2079
	C3	250	250	2175	300	300	2241	350	350	2435
	C4	250	250	2687	300	300	2815	350	350	2797
11-15	C1	250	250	2000	250	250	1935	250	250	1944
	C2	250	250	1975	250	250	2000	250	250	2100
	C3	250	250	2193	250	250	2185	250	250	2155
	C4	250	250	2106	250	250	2375	250	250	2365

the allowable value. The lateral story drift ratios from the 4th to 15th floors are very close to the allowable values in *y* direction, which indicates that the elastic drift responses can be improved by the OC procedure by resizing the member sections.

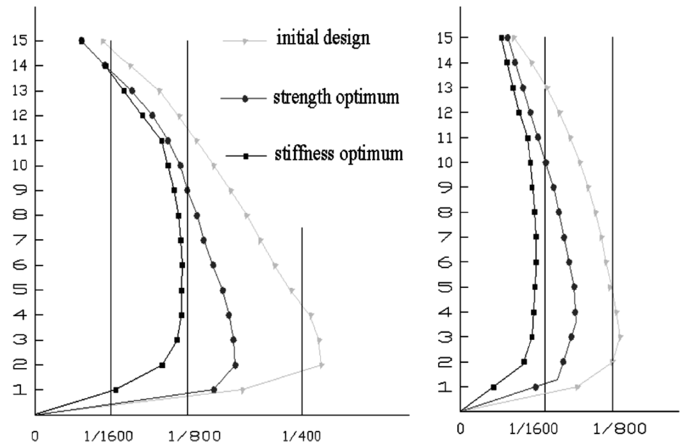

Fig. 6 Inter-story drifts in *y* direction and *x* direction under earthquake load

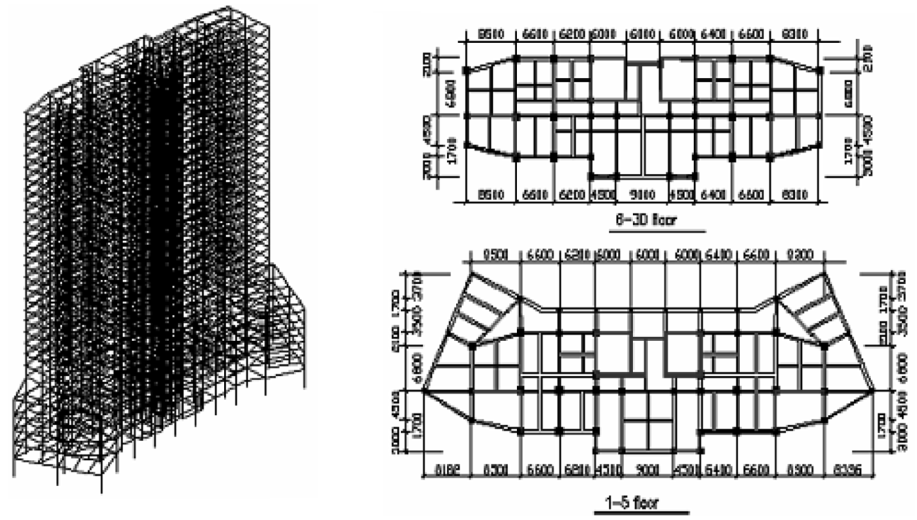

Fig. 7 Vertical plan and standard story layout

5.2 A 30-story frame shear wall structure

This example is a practical frame-shear wall structure (Fig. 7), with the total height of 97.5 m, the story height of 4.5 m for the lower five stories, and 3.0 m for other stories. There are three stories under ground with the area of 4485 m^2, and 30 stories above the ground with the area of 35210 m^2. 1-5 stories are designed for office and 6-30 stories for residence. The building is divided into four standard levels, 1-5 stories, 6-10 stories, 11-25 stories and 26-30 stories. The building is located in the coastal site with the standard wind pressure of 0.75 kN/m^2, and the wind load is dominant factor in the design. Due to the function requirements of the building, the shear walls are distributed in the middle part and two sides. The concrete compression strength fc is 16.7 Mpa and the steel reinforcement strength fy is 300 Mpa for all members. The allowable elastic inter-story drift ratio is 1/800. The allowable range of the column axial compression ratio is between 0.5 and 0.6 and the allowable range of beam reinforcement ratio is between 0.25% and 2.0%. The column is assumed to square-shaped and the width for all beams and walls is fixed. The cost of concrete, steel, and formwork is estimated as C_c = 100 US$/m^3, C_s = 550 US$/ton, and C_f = 1.6 US$/m^2, respectively. Based on the initial design, we redesign this building using the above SA-OC method.

It is known that the axial compression ratio is an important index for the strength capacity and ductility of the column. A column with a smaller axial compression ratio is conservative in design, while a column with a larger one is poor in ductility. In the initial design, the axial compression ratio of columns are between 0.25 and 0.7, and the column depths are between 450 mm and 1000 mm, as shown in Fig. 8 and Fig. 9. The big difference in the axial compression ratios of columns resulted in the poor mechanical properties of the initial structure. In the optimum design, the axial compression ratios of columns are located between 0.5 and 0.6 and the column depths are between 300 mm and 850 mm. These results mean that the optimum design can save the material and improve the structural properties as well.

Fig. 10 and Fig. 11 list the section depth and reinforcement ratio of the optimized beams in the first standard level. In the initial design, the beam reinforcement ratios are distributed between 0.25% and 1.1%, and the beam depths are distributed between 350 mm and 750 mm. It is found that some beams with the reinforcement ratio of 0.25% (the lower bound specified by the design

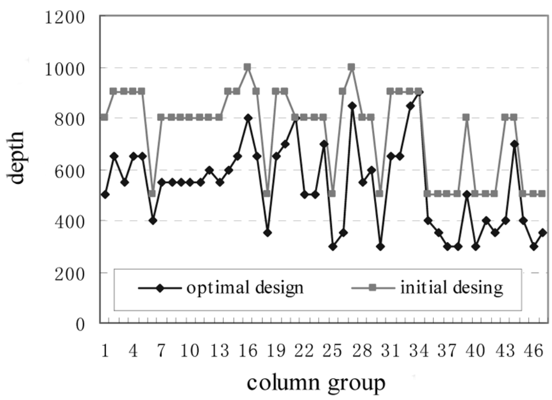

Fig. 8 Column axial compress ratio displacement

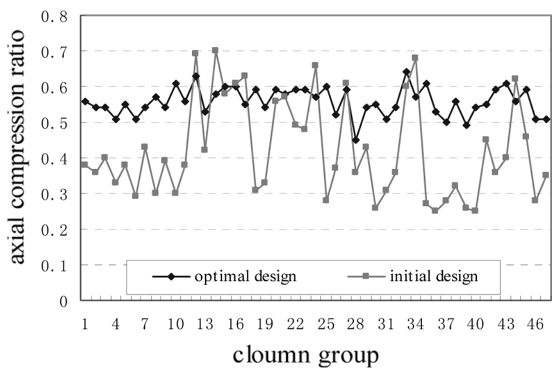

Fig. 9 Column depth displacement

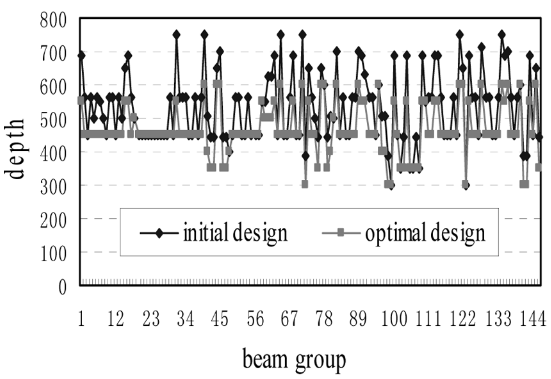

Fig. 10 Beam depth displacement

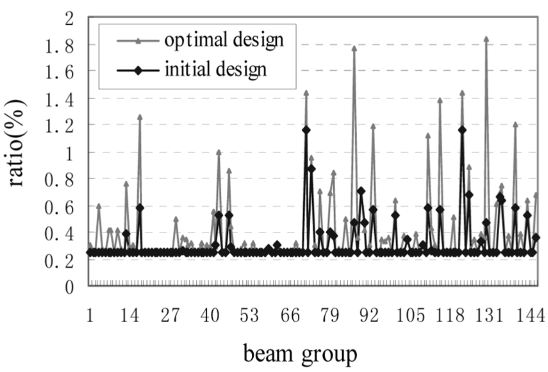

Fig. 11 Beam reinforcement ratio displacement

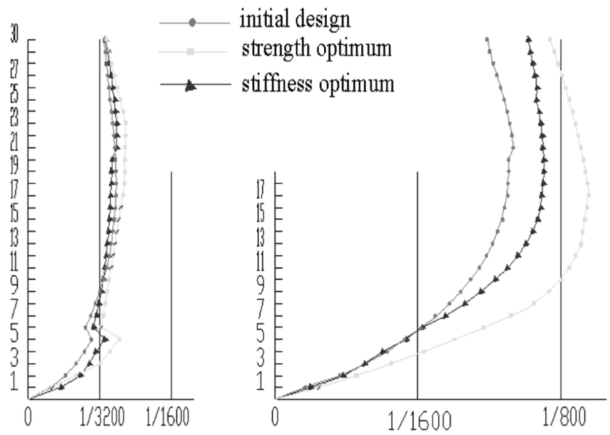

Fig. 12 Inter-story drifts in *x* direction and *y* direction under earthquake load

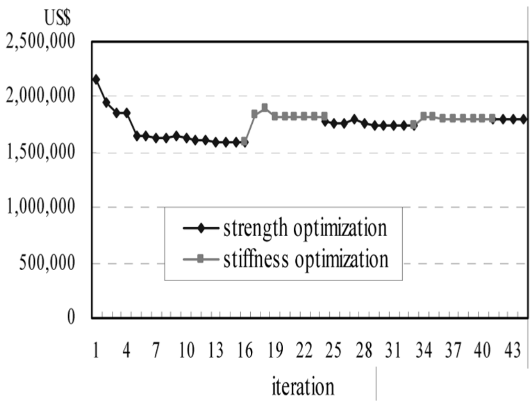

Fig. 13 Optimization history

code) have larger section size, which increase the material cost and decrease the usable space of the structure. In the optimum design, the section depths of some beams are reduced, distributed between 300 mm and 600 mm; the beam reinforcement ratios are increased slightly, located between 0.25% and 1.8%. It is also found that there are still some beams with the section size of the initial design, which are needed to satisfy the requirements of shear-resistant capacity and maximum crack width.

Fig. 12 presents the inter-story drift ratios of the initial design, strength optimal design, and stiffness optimal design, respectively. As shown in Fig. 12, in the initial design, the maximum story-drift ratios in *x* and *y* direction are far less than the allowable value of 1/800 due to the larger member section size. After the strength optimization, the maximum drift ratio in *x* direction is changed slightly, but the maximum drift ratio in *y* direction increases a lot and violates the allowable value. Finally, after stiffness optimization, the structure members are resized and the maximum story drift ratio in *y* direction satisfies the allowable value.

A steady convergence to the optimal design is shown evidently in Fig. 13. After optimization, the structure cost decreases from US$ 2167216 to US$ 1802180, reduced by 15%. In addition, the maximum depth of beam in the optimum design is reduced from the original 750 mm to 600 mm, which makes the net space in height of each story enlarged. In other words, if the net space in height of each story keeps the same as the initial design, then one more story can be added to the building after the optimum design, with the total height of the building unchanged, by which, the usable floor area will increase by 3.32%.

6. Conclusions

A practical optimum design procedure of a hybrid SA-OC method is proposed in this paper, to optimize the component dimensions and reinforcement of RC frames under multi-loads according to Chinese design codes. The procedure minimizes the total cost of the reinforced concrete structure while satisfying the strength and stiffness constraints. The hybrid SA-OC method combines the advantages of both SA and OC methods, involving the strength optimum design by SA algorithm and stiffness optimum design using OC method. An adaptive feasible region technique based on the axial compression ratio, reinforcement ratio and local strength constraints is developed to improve the efficiency of SA, which makes the SA capable of optimization design of the complicated building structures. The strength optimal design procedure is linked to building structure design software SATWE and the stiffness optimal design procedure to ANSYS. Thus the hybrid SA-OC method proposed in this paper has attractive practicality, feasibility and applicability as a powerful computer-based technique of optimum design for RC frame structures under multi-load cases.

Acknowledgements

The support of the National Natural Science Foundation of China (No. 90815023 and No. 10721062), the National Basic Research Program of China (973 Program, 2006CB705403) is much appreciated.

References

Aarts, E.H.L. and van Laarhoven, P.J.M. (1987), *Simulated Annealing: Theory and Application*, D Reidel Publishing Company, Dordrecht.

Aschheim, M., Hernndez-Montes, E. and Gil-Martn, L.M. (2007), "Optimal domains for strength design of rectangular sections for axial load and moment according to Eurocode 2", *Eng. Struct.*, **29**(8), 1752-1760.

Balling, R.J. and Yao, X. (1997), "Optimization of reinforced concrete frames", *J. Struct. Eng-ASCE*, **123**(2), 193-202.

Chan, C.M. and Zou, X.K. (2004), "Elastic and inelastic drift performance optimization for reinforced concrete building under earthquake loads", *Earthq. Eng. Struct. D.*, **33**, 929-950.

Chan, C.M. and Sun, S.L. (1997), "Optimal drift design of tall reinforced concrete building frameworks", *Adv. Struct. Optim.* (Eds. Frangopol, D.M. and Cheng, F.Y.), American Society of Civil Engineers, New York.

Chan, C.M. (2001), "Optimal lateral stiffness design of tall building of mixed steel and concrete construction", *Struct. Des. Tall Build.*, **10**(3), 155-177.

Chen, J.J., Che, J.W., Sun, H.A., Ma, H.B. and Cui, M.T. (2002), "Structural dynamic optimization with probability constraints of frequency and mode", *Struct. Eng. Mech.*, **13**(5), 479-490.

Cheng, G.D., Li, G. and Cai, Y. (1998), "Reliability-based structural optimization under hazard loads", *Struct. Optim.*, **16**, 128-135.

Ferreira, C.C., Barros, M.H.F.M. and Barros, A.F.M. (2003), "Optimal design of reinforced concrete T-sections in bending", *Eng. Struct.*, **25**, 951-964.

Gong, Y., Xu, L. and Grierson, D.E. (2005), "Performance-based designsensitivity analysis of steel moment frames under earthquake loading", *Int. J. Numer. Meth. Eng.*, **63**, 1229-1249.

Guan, H. (2005), "Strut-and-tie model of deep beams with web openings- An optimization approach", *Struct. Eng. Mech.*, **19**(4), 361-379.

Hernndez-Montes, E., Aschheim, M. and Gil-Martn, L.M. (2004), "The impact of optimal longitudinal reinforcement on the curvature ductility capacity of reinforced concrete column sections", *Mag. Concrete Res.*, **56**(9), 499-512.

Hernndez-Montes, E., Gil-Martn, L.M. and Aschheim, M. (2005), "The design of concrete members subjected to uniaxial bending and compression using reinforcement sizing diagrams", *ACI Struct. J.*, **102**(1), 150-158.

Jasbir, S.A. (1997), "Guide to structural optimization", *ASCE Manual and Reports on Engineering Practice No.90*, 165-196.

Kirpatrick, S., Gelatt, C.D. and Vecchi, Jr., M. (1983), "Optimization by simulated annealing", *Science*, **220**, 671-681.

Li, G., Zhou, R.G., Duan, L. and Chen, W.F. (1999), "Multi-objective and multilevel optimization for steel frames", *Eng. Struct.*, **21**(6), 519-529.

Metropolis, N., Rosenbluth, A., Rosenbluth, M., Teller, A. and Tell, E. (1953), "Equations of state calculation by fast computing machines", *J. Chem. Phys.*, **21**(6), 1087-1092.

Mohan, R.A. and Arvind, N. (2007), "Optimal stacking sequence design of laminate composite structures using tabu embedded simulated annealing", *Struct. Eng. Mech.*, **25**(2), 239-268.

National Standard of the People's Republic of China (2001), *Chinese Code for Seismic Design Buildings (GB 50011-2001)*, Chinese Building Industry Press, Beijing, China.

National Standard of the People's Republic of China (2002), *Chinese Code for Concrete Design Buildings (GB 50010-2002)*, Chinese Building Industry Press. Beijing, China.

Pantelides, C.P. and Tzan, S.R. (1997), "Optimal design of dynamically constraint structures", *Comput. Struct.*, **62**(1), 141-149.

Park, H.S. and Hong, K. (2002), "Drift design of steel-frame shear-wall system for tall buildings", *Struct. Des. Tall Spec. Build.*, **11**, 35-49.

Park, H.S. and Kwon, J.H. (2003), "Optimal drift design model for multi-story buildings subjected to dynamic lateral forces", *Struct. Des. Tall Spec. Build.*, **12**, 317-333.

Park, H.S. and Sung, C.W. (2002), "Optimization of steel structure using distributed simulated annealing algorithm on a cluster of personal computer", *Comput. Struct.*, **80**, 1305-1316.

Parks, G.T. (1990), "An intelligent stochastic optimization routine for nuclear fuel cycle design", *Nucl. Technol.*, **89**(2), 233-246.

Zou, X.K., Chan, C.M., Li, G. and Wang, Q. (2007), "Multi-objective optimization for performance-based design of reinforced concrete frames", *J. Struct. Eng-ASCE*, **133**(10), 1462-1774.